Articles

Cardiotoxin II Segregates Phosphatidylglycerol from Mixtures with Phosphatidylcholine: ^{31}P and ^{2}H NMR Spectroscopic Evidence†

Mary Anna Carbone and Peter M. Macdonald*

Department of Chemistry and Erindale College, University of Toronto, Toronto, Ontario, Canada M5S 1A2

Received October 2, 1995; Revised Manuscript Received January 10, 1996⊗

ABSTRACT: The interaction of the cationic protein cardiotoxin II (CTX II) with mixtures of zwitterionic 1-palmitoyl-2-oleoyl-*sn*-glycero-3-phosphocholine (POPC) and anionic 1-palmitoyl-2-oleoyl-*sn*-glycero-3-phosphoglycerol (POPG) was investigated using phosphorus (^{31}P) and deuterium (^{2}H) nuclear magnetic resonance (NMR) spectroscopy. Adding CTX II to 1:1 POPC/POPG mixtures produced a two-component ^{31}P NMR spectrum, in which the second component had a decreased chemical shift anisotropy. Simultaneously, the ^{2}H NMR quadrupolar splitting measured from both POPC-α-d_2 and POPC-β-d_2 decreased. Thus, CTX II produces an altered macroscopic phase state of the lipid bilayers, and this obscures any effects on bilayer surface electrostatics observed by ^{2}H NMR. Using magic angle spinning (MAS) ^{31}P NMR spectroscopy, two isotropic resonances were resolved in the absence of CTX II and were assigned to POPG (0.47 ppm) and POPC (−0.58 ppm). Adding CTX II produced two new isotropic resonances shifted approximately 0.5 ppm downfield. Quantifying the intensities of the various resonance lines revealed that the binding isotherms for different POPC/POPG mixtures shifted onto a universal curve when expressed as a function of the CTX II/POPG ratio. The results indicate that CTX II binds preferentially to POPG and is able to laterally segregate POPG from POPC. Fitting of the binding isotherms was achieved using a two-site model derived from statistical-thermodynamic considerations. One class of binding site is specific for POPG and the other is nonspecific, capable of binding both POPC and POPG.

Cardiotoxin II (CTX II) is a major component of the venom from the cobra *Naja mossambica mossambica.* It is a 60 amino acid, lytic protein, capable of inducing heart failure, depolarizing muscular and nerve cells, and causing cytolysis and hemolysis (Harvey *et al*., 1982). CTX II shares important structural features in common with other lytic proteins, like snake myotoxin and bee mellitin, in that it is rich in hydrophobic and cationic amino acid residues which are grouped to form hydrophic-rich and cationic-rich domains in the folded protein (Rees & Bilwes, 1993). CTX II is unusual, however, in that its hydrophobic and cationic domains are distributed amongst three loops of β-pleated sheet. These radiate from a central core and are cross-linked and held in place by four disulfide bridges (Singhal *et al*., 1993). The extremity of one loop is completely hydrophobic, with cationic residues located at the fringes of the hydrophobic cluster (Rees & Bilwes, 1993).

It is postulated that the cationic residues of CTX II interact with anionic phospholipids in the polar headgroup region at the membrane surface, while its hydrophobic clusters penetrate to the interior of the lipid bilayer (Bougis *et al*., 1981; Dufourcq *et al*., 1982). The electrostatic associations seem to have primacy, since CTX II interacts preferentially and stoichiometrically with negatively charged lipids (Dufourq & Faucon, 1978; Vincent *et al*., 1978). These interactions are strong enough that CTX II is able to laterally segregate phosphatidic acid from within a phosphatidic acid/phosphatidylcholine mixture (Désormeaux *et al*., 1992). When added to cardiolipin bilayers, CTX II induces the formation of inverted CTX II/cardiolipin micelles, with CTX II located in the interior of the inverted micelles (Batenburg *et al*., 1985).

The hydrophobic interactions are not, however, insignificant. Recent ^{1}H NMR studies indicate that CTX II can in fact bind strongly to both anionic and zwitterionic lipids (Chien *et al*., 1994; Dauplais *et al*., 1995). Insertion of the hydrophobic domains into the bilayer interior, whether this changes the native conformation of CTX II (Surewicz *et al*., 1988) or not (Pézolet *et al*., 1982), certainly contributes to the high affinity of CTX II for lipid bilayers.

Given the advanced state of our understanding of CTX II−phospholipid interactions, it should be possible to pose further fundamental questions regarding CTX II−phospholipid interactions in particular and protein−lipid interactions in general. One specific issue is whether CTX II can laterally segregate monovalent anionic lipids. This question arises when one notes that cardiolipin is a divalent anionic phospholipid, while phosphatidic acid exists as a mixture of monovalent and divalent anionic species at physiological pH and forms less-than-ideal mixtures with phosphatidylcholine (Nikolelis *et al*., 1992). Another specific issue is whether

† This research was supported by a National Science and Engineering Research Council of Canada Operating Grant (P.M.M.).

* To whom correspondence should be addressed. Telephone: 905-828-3805. Fax: 905-828-5425. E-mail: pmacdona@credit.erin.utoronto.ca.

⊗ Abstract published in *Advance ACS Abstracts,* February 15, 1996.

0006-2960/96/0435-3368$12.00/0

any segregated phase which results must necessarily assume an inverted micelle architecture. Cardiolipin, for example, readily forms a nonbilayer phase (Seelig, 1978). Thus, it would be informative to examine the interactions of CTX II with a monovalent anionic phospholipid which mixes ideally with phosphatidylcholine and has little inherent tendency to assume a nonbilayer macroscopic phase structure. One such phospholipid is phosphatidylglycerol. Yet another issue is whether any segregated phase induced by CTX II contains exclusively anionic lipids versus a mixture of lipids, and how the phase composition may be described in theoretical terms.

In this article we report static and MAS (magic angle spinning) ^{31}P NMR plus broad-line ^{2}H NMR measurements on mixed phosphatidylglycerol/phosphatidylcholine lipid bilayers exposed to CTX II. Static ^{31}P NMR measurements provide a picture of the macroscopic architecture of phospholipid assemblies, i.e., bilayer versus hexagonal H_{II} versus isotropic arrangements, (Seelig, 1978). MAS ^{31}P NMR can be used to quantify specific protein−phospholipid interactions, as demonstrated recently by Pinheiro and Watts (1994) in their innovative study of the cationic, surface-binding protein, cytochrome *c*, bound to mixed cardiolipin/phosphatidylcholine/phosphatidylethanolamine bilayers. ^{2}H NMR of specifically choline-deuterated phosphatidylcholine can be used to monitor lipid bilayer surface electrostatic charge (Seelig *et al*., 1987). The technique can also differentiate ideal versus laterally phase-separated mixtures (Marassi & Macdonald, 1992; Marassi *et al*., 1993).

Here, we combine all three of these techniques to examine the ability of CTX II to laterally segregate phosphatidylglycerol from mixtures with phosphatidylcholine. We demonstrate that indeed separate phase domains are induced by CTX II in such phospholipid mixtures, and that the segregated phase is enriched with phosphatidylglycerol but does not exclude phosphatidylcholine. Moreover, it retains an overall lamellar organization. We show, further, that the phase composition may be described in statistical-thermodynamics terms using a model of CTX II−phospholipid interactions involving two classes of phospholipid binding site, one highly specific for phosphatidylglyerol and the other nonspecific and able to accomodate either phosphatidylglycerol or phosphatidylcholine.

MATERIALS AND METHODS

Synthesis of Choline Deuterated POPC. The following nomenclature is employed to indicate deuteron positions in the phosphocholine headgroup of phosphatidylcholine:

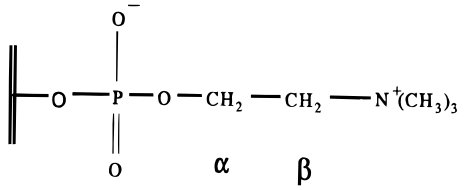

Nondeuterated lipids were purchased from Avanti Polar Lipids (Alabaster, AL). Choline was selectively deuterated at the α- and β-segments by a combination of the methods described by Harbisson and Griffith (1984) and Aloy and Rabaut (1913). POPC-α-d_2 and POPC-β-d_2 were prepared by coupling 1-palmitoyl-2-oleoyl-*sn*-glycero-3-phosphate (POPA) with choline tetraphenylboron salt, selectively deuterated at the α or β segment, using 2,4,6-triisopropylbenzenesulfonyl chloride (TPS) as the condensing agent (Aneja *et al*., 1970). The choline-deuterated phosphatidylcholines were purified by chromatography on Amberlite mixed bed ion exchange resin (BDH, Mississauga, ON) followed by acetone precipitation (Kates, 1972). The purity of the synthesized lipids was evaluated by thin layer chromatography (TLC) and ^{1}H NMR. All final products resulted in a single spot on a overloaded TLC plate, migrating with an R_F identical to that of authentic POPC. The ^{1}H NMR spectra were identical to that of nondeuterated POPC, except for the changes expected in the presence of α- or β-deuterons.

Isolation of Cardiotoxin II. CTX II [equivalent to V_2II of Louw (1974)] was isolated from the venom of *N. mossambica mossambica* (Sigma, St. Louis, MO) as outlined by Karlsson *et al*. (1971) and Fryklund and Eaker (1975). Dried crude venom (200 mg) was dissolved in 2 mL of 0.2 M ammonium acetate, pH 7.3. Venom components were separated on a 2 cm × 55 cm column of Sephadex G-75 by elution in the same medium. Fractions were monitored by UV absorption at 280 nm, and those containing cardiotoxin-like characteristics were pooled and lyophilized. CTX II was separated from other cardiotoxins using cation exchange chromatography on Bio-Rex-70, 400 mesh (Bio-Rad, Mississauga, ON) eluted with a 2−1 concave gradient of 0.11 versus 1.5 M ammonium acetate. Putative CTX II-containing fractions were subjected to fluorescence and UV absorption measurements using an SLM model 4800 Fluorometer. Fractions with fluorescence (excitation wavelength 280 nm; emission maxima 350 nm) and UV spectra ($E_{280}^{0.1\%} = 1.385$) characteristic of CTX II (Bougis *et al*., 1986) were tested for purity using sodium dodecyl sulfate−polyacrylamide gel electrophoresis (SDS−PAGE) on a 25% gel. Fractions running as a single band with a molecular mass of about 6000 Da were pooled and desalted using Sephadex G-25 chromatography. The identity of CTX II was verified using amino acid compositional analysis performed by the Biotechnology Service Centre of the Hospital for Sick Children and the Department of Clinical Biochemistry, University of Toronto. From the original 200 mg of dried cobra venom, we obtained approximately 50 mg of purified CTX II.

Sample Preparation. Aqueous mixtures of POPC/POPG/CTX II were prepared for NMR spectroscopy as follows. POPC-α-d_2 or POPC-β-d_2 (15 mg, 19.7 μmol) plus the desired amount of POPG were mixed by combining appropriate volumes of chloroform stock solutions. The solvent was then removed by evaporation under a stream of argon gas followed by exposure to high vacuum overnight. The dried lipids were hydrated and dispersed in a minimal volume (100−150 μL) of saline buffer (150 mM NaCl, 10 mM EDTA, pH 6.5) containing the desired amount of CTX II. Homogeneous mixing was ensured by a sequence of five cycles of freeze−thaw (freezing in liquid nitrogen and heating to 40 °C in a water bath, with intermittent vortexing). Samples for ^{2}H NMR were transferred to a 5 mm glass sample vial and sealed. Samples for ^{31}P NMR were transferred to a 5.89 mm (outside diameter) × 0.8 mm (wall thickness) × 8 mm (length) pyrex precision bore tube (Wilmad, Buena, NJ) which was then sealed at both ends with a rubber stopper epoxied in place.

To assess the level of CTX II binding to the phospholipid multilamellar vesicles, certain lipid dispersions were centrifuged and the clear supernatant was recovered. No CTX II

could be detected in any of these supernatants using UV or fluorescence techniques, even at the highest levels of CTX II added. We conclude that CTX II binds quantitatively to these phospholipid bilayer membranes at all concentrations employed here.

^{31}P NMR Spectroscopy. Proton-decoupled ^{31}P NMR (static and MAS) spectra were recorded using a Chemagnetics CMX300 spectrometer equipped with a Chemagnetics MAS probe doubly tuned to the resonance frequency of phosphorus-31 (121.254 MHz) and protons (299.53 MHz). Samples prepared as described above were spun in a 7.5 mm o.d. zirconium rotor at a predetermined, digitally monitored spinning rate. For MAS spectra, a single excitation pulse was employed (90° pulse width, 6.5 μs) with proton decoupling during acquisition (50 kHz proton decoupling field strength), complete quadrature phase cycling, and a recycle delay of 2 s. Typically, 5000−14 000 acquisitions of 4K time domain points spanning a spectral width of 50 kHz were collected, zero-filled to 8K points, multiplied by a decaying exponential corresponding to a line broadening of 5 Hz, and processed by Fourier transformation. Static spectra were acquired using a Hahn echo pulse sequence with phase cycling of the pulses and proton decoupling as described by Rance and Byrd (1983). Specifics regarding acquisition parameters additional to or different from those mentioned above, including the interpulse delay (40 μs), the spectral width (250 Hz), and the number of acquisitions (6000) are again noted in parentheses. Phosphorus-31 spin−lattice (T_1) relaxation times were measured using an inversion−recovery pulse sequence [180°−τ−90°−acq], with proton decoupling and a recycle delay of 15 s. Fast MAS ^{31}P NMR spectra were simulated using FELIX for Windows 1.0.

^{2}H NMR Spectroscopy. ^{2}H NMR spectra were recorded on a Chemagnetics CMX300 NMR spectrometer operating at 45.98 MHz employing the quadrupolar echo technique (Davis *et al*., 1976) and using quadrature detection with complete phase cycling of the pulse pairs (Griffin, 1981). Specifics regarding the 90° pulse length (2.5 μs), the interpulse delay (40 μs), and the recycling delay (100 ms) are those noted in parentheses. Typically, 30 000−100 000 acquisitions of 1K time domain points spanning a spectral width of 250 kHz were collected, multiplied by a decaying exponential corresponding to a line broadening of 100 Hz, and processed by Fourier transformation.

RESULTS AND DISCUSSION

CTX II Induces a Distinct Phospholipid Phase in POPG/POPC Mixtures. CTX II is known to produce an isotropic micellar phase when added to cardiolipin (CDL) bilayers, an effect readily observed via ^{31}P NMR (Batenburg *et al*., 1985). A similar effect is observed with POPG mixed with POPC as demonstrated in Figure 1.

Figure 1A shows static ^{31}P NMR spectra of 1:1 (mol/mol) mixtures of POPC/POPG as a function of increasing CTX II (from bottom to top). In the absence of CTX II the static ^{31}P NMR spectrum (bottom spectrum) consists of a powder pattern line shape, having an apparent residual chemical shift anisotropy ($\Delta\sigma = \sigma_{\parallel} - \sigma_{\perp}$) equal to 38 ppm and an asymmetry parameter (η) close to zero. This spectral line shape is diagnostic of fluid phospholipids in a liquid-crystalline bilayer. The observed $\Delta\sigma$ for such a 1:1 POPC/POPG mixture is reduced relative to the value of 42 ppm measured for 100% POPC due to the well-known "molecular voltmeter" effect operative in the presence of charged (in this case anionic) species at the bilayer interface (Seelig *et al*., 1987). Of course, the spectrum is a superposition of two powder patterns, originating with the phosphorus nuclei of POPC and POPG. The two powder patterns are not

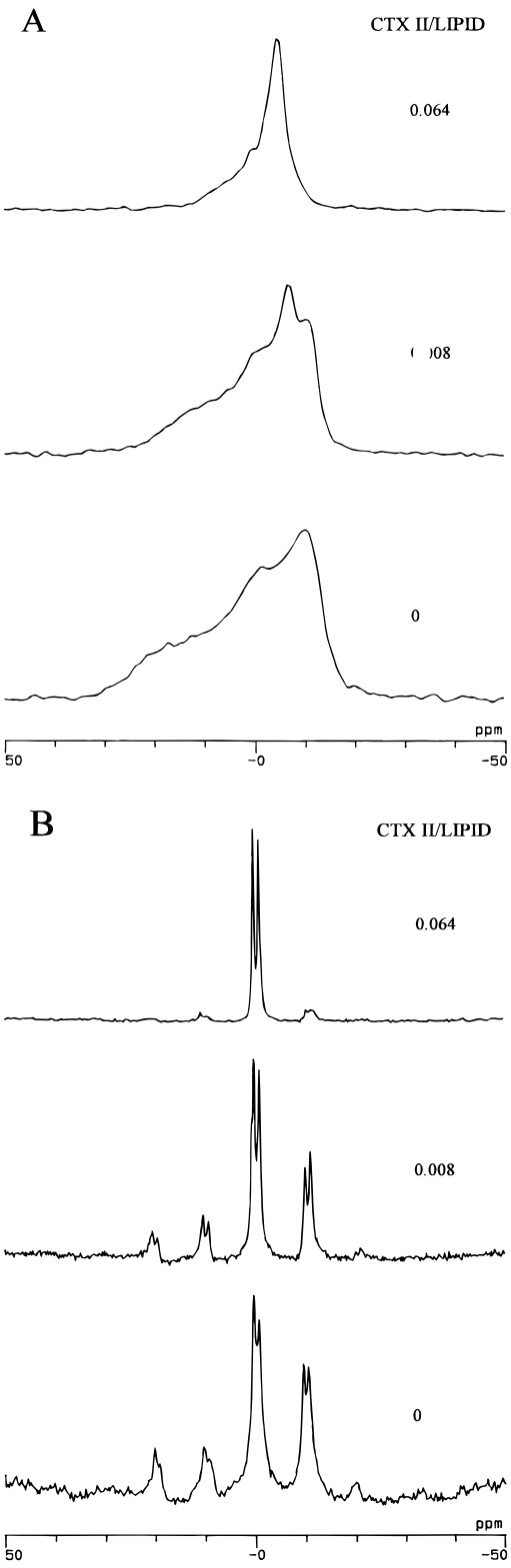

FIGURE 1: (A) Representative static ^{31}P NMR spectra from 1:1 POPC/POPG mixtures in the presence of the following molar ratios of CTX II/total lipid, from bottom to top: 0, 0.8, and 6.4 mol %. (B) Corresponding slow-spinning MAS ^{31}P NMR spectra (frequency of rotation = 1200 Hz).

Table 1: ^{31}P NMR Chemical Shift Anisotropies and T_1 Relaxation Times for Mixtures of POPC/POPG (1:1) plus CTX II in the "Free" versus "Bound" States

CTX II/total lipid (mol %)[a]	isotropic chemical shift σ (ppm)[b]	anisotropic chemical shift $\Delta\sigma$ (ppm)	T_1 relaxation time (s)
	POPG		
0	0.5	42	1.4
3.2	1.0	16	1.4
	POPC		
0	−0.6	38	1.6
3.2	−0.1	14	1.2

[a] 0 mol % CTX II equals the 100% "free" and 3.2 mol % CTX II equals the 100% "bound" state. [b] Referenced to 85% H_3PO_4.

precisely identical but are not readily resolved in the static case.

The corresponding slow-spinning MAS ^{31}P NMR spectrum, shown in figure 1B (bottom spectrum), breaks up into a pair of isotropic resonances plus their attendant spinning side bands (SSBs). The low-field isotropic resonance is assigned to POPG and the high-field resonance to POPC. The SSBs are separated from the isotropic resonances by multiples of the MAS frequency. Their intensities reflect the envelope of chemical shifts manifest in the static spectra and may be analyzed to obtain the particular residual chemical shift anisotropies and asymmetry parameters, as described by Herzfeld and Berger (1980) and listed in Table 1 for the cases discussed here. It is evident, for example, that both POPG and POPC have similar values of $\Delta\sigma$ despite the approximately 1.1 ppm difference in their isotropic chemical shifts.

Adding 6.4 mol % CTX II causes a reduction of $\Delta\sigma$ to a value of 16 ppm, as evident by the reduced width of the static ^{31}P NMR spectrum (top spectrum, Figure 1A). The entire phospholipid population, both POPG and POPC, experiences the effects of CTX II at this concentration, since there is no evidence in the spectrum of any population of phospholipids having $\Delta\sigma$ equal to 38 ppm, while further additions of CTX II result in no further change to the static ^{31}P NMR spectrum. It is noteworthy that CTX II does not reduce $\Delta\sigma$ to zero for the 1:1 POPC/POPG mixture, unlike the situation for CDL where CTX II addition produces an isotropically averaging ($\Delta\sigma \sim 0$) lipid component (Batenburg *et al*., 1985). Small-angle X-ray diffraction studies by these same workers confirmed that CTX II and CDL together assume an inverted micellar architecture. The static ^{31}P NMR results obtained here suggest that CTX II/POPC/POPG mixtures assume an architecture different in detail from that of CTX II/CDL mixtures. One may rationalize the difference as being due to the bilayer stabilizing influence of POPC and POPG versus the propensity of CDL to form nonbilayer phases.

In the slow-spinning MAS ^{31}P NMR spectrum of 1:1 POPC/POPG mixtures in the presence of 6.4 mol % CTX II (top spectrum, Figure 1B), the SSBs intensity is virtually lost and only the isotropic chemical shift components remain. This indicates that the rate of sample spinning, although slow relative to $\Delta\sigma$ for POPC and POPG in the absence of CTX II, is fast relative to $\Delta\sigma$ for these lipids in the presence of 6.4 mol % CTX II. For both POPC and POPG, these isotropic resonances are in fact shifted downfield by approximately 0.5 ppm relative to their values in the absence of CTX II.

Adding an intermediate amount of CTX II (0.8 mol %) produces a static ^{31}P NMR spectrum which consists of a superposition of two powder patterns (middle spectrum, Figure 1A). One component manifests a value of $\Delta\sigma$ corresponding to that measured in the absence of CTX II. The second has a value of $\Delta\sigma$ corresponding to that measured in the presence of 6.4 mol % CTX II. This indicates that two phospholipid phases are present simultaneously and that they are in slow exchange with one another on the the NMR timescale. One phase must be free of CTX II and the other CTX II-enriched. Although in principle the quantity and composition of the two phases can be obtained from such static ^{31}P NMR spectra, given the limited resolution plus the fact that both POPC and POPG contribute phosphorus resonances to the observed spectrum, such an analysis is impractical.

The slow MAS ^{31}P NMR spectrum for 0.8 mol % CTX II, shown in Figure 1B (middle spectrum), also indicates the presence of two separate phospholipid environments in slow exchange with one another, one having a value of $\Delta\sigma$ much reduced relative to the other. In particular, the addition of CTX II reduces the intensities of the SSBs relative to those of the isotropic resonances. However, the intensity ratios of the SSBs relative to one another remain constant. For instance, the ratio of the n_{-1} to the n_{+1} SSB intensities is approximately 2.7 for both POPG and POPC in the absence of CTX II and 2.6 in the presence of 0.8 mol % CTX II. Likewise, the intensity ratio for the n_{+1} and the n_{+2} SSBs is more-or-less conserved upon the addition of 1 mol % CTX II. On the other hand, if there were fast exchange between the two phospholipid phases, then the observed $\Delta\sigma$ would be an average of the corresponding values of the two phases. This would alter the intensity ratios for different sets of SSBs, in particular for the intensity ratio (n_{+1}/n_{+2}).

From such slow-spinning MAS ^{31}P NMR spectra one may extract semiquantitative information regarding the amount and composition of the two phospholipid phases. The amount of a given phospholipid in a given phase is represented by the sum of the integrated intensities of its SSB plus its isotropic resonance line. To a good approximation, the slow-spinning MAS ^{31}P NMR spectrum with excess CTX II consists solely of isotropic resonances with no SSB intensity of consequence. In the absence of CTX II the isotropic POPG and POPC resonances have a fixed intensity relative to their corresponding SSBs provided the rate of sample spinning is fixed. Therefore, at intermediate CTX II concentrations, the integrated SSB intensity arises solely from the phospholipid phase free of CTX II, while the integrated intensity of the isotropic resonance lines arises due to the sum of the isotropic resonances of the two phases. From such a calculation one estimates that at this CTX II concentration roughly 15−20 mol % of the POPC/POPG mixture is involved in the CTX II-induced phase. This suggests further, given the particular CTX II/POPG/POPC mole ratio, that an individual CTX II molecule interacts with about 15−20 phospholipids. Finally, one notes that CTX II causes the n_{-1} SSB intensity for POPG to decrease relative to POPC. This hints that the CTX II-induced phase is enriched with POPG versus POPC. However, other SSBs show no such clear-cut effect. Given the signal-to-noise ratio in these spectra, any attempt to quantify the degree of enrichment by scrutinizing the SSBs intensities would be imprudent. A better approach is to employ fast MAS ^{31}P

NMR in order to maximize signal-to-noise and spectral resolution.

The ^{2}H NMR "Molecular Voltmeter" Technique and CTX II. ^{2}H NMR of specifically choline-deuterated POPC can be used to quantify lipid bilayer surface electrostatics (Seelig *et al*., 1987). Since CTX II−bilayer interactions are largely mediated by electrostatic interactions, it is important to examine whether the so-called deuterium "molecular voltmeter" can be applied to the case of CTX II.

The effects of CTX II on the ^{2}H NMR spectra from 1:1 POPC-α-d_2/POPG and POPC-β-d_2/POPG mixtures are shown in Figure 2, panels A and B, respectively. In the absence of CTX II (bottom spectra), the ^{2}H NMR spectra are typical Pake doublets, characteristic of liquid-crystalline lipids in a bilayer arrangement. The quadrupolar splitting ($\Delta\nu$) corresponds to the separation (in Hz) between the two maxima in the ^{2}H NMR spectrum. For the case of POPC-α-d_2 (POPC-β-d_2) mixed 1:1 with POPG, $\Delta\nu$ equals 10.0 kHz (1.8 kHz), which is larger (smaller) than the value measured with bilayers composed of 100% POPC. This counterdirectional change in the size of the quadrupolar splitting at the α- versus β-deutero-labeling position is characteristic of the "molecular voltmeter" response of the choline headgroup to membrane surface charge. The direction of the change observed here in the presence of 50 mol % POPG, i.e., $\Delta\nu$ increases for POPC-α-d_2 and decreases for POPC-β-d_2, is precisely that expected due to anionic surface charges.

Increasing the CTX II concentration (from bottom to top in the figure) has the effect of decreasing $\Delta\nu$ for both POPC-α-d_2 and POPC-β-d_2. At the higher CTX II concentrations, the spectra for POPC-α-d_2 retain a visible quadrupolar splitting, while the spectra for POPC-β-d_2 collapse to a broad ill-defined line shape with no visible quadrupolar splitting. For either deutero-labeling position, the decrease in $\Delta\nu$ is approximately linear with increasing CTX II.

The effects of CTX II on the ^{2}H NMR spectra are clearly different from the effects observed in the ^{31}P NMR spectra where CTX II induces the appearance of the second spectral component. Despite the fact that ^{31}P and ^{2}H NMR operate on similar time scales, no distinct second spectral component can be resolved with certainty in the ^{2}H NMR spectra in Figure 2A,B. One may understand this difference between the ^{31}P NMR and the ^{2}H NMR results in terms of the combined effects of surface electrostatics and molecular order. In lipid bilayers, ^{31}P NMR reports primarily on the macroscopic organization of the bilayer lipids. ^{2}H NMR of choline-deuterated POPC, on the other hand, reports on a combination of both influences. The sensitivity of the "molecular voltmeter" response of POPC becomes muted when lipid disorder increases (Macdonald *et al*., 1991), so that order−disorder considerations can outweigh electrostatic considerations in producing the net quadrupolar splitting. According to the ^{31}P NMR evidence, POPC trapped within a CTX II-bound phase is relatively disordered overall, which will decrease ^{2}H NMR quadrupolar splittings regardless of deutero-labeling position. As to the surface electrostatic response of the ^{2}H NMR quadrupolar splittings, it is not certain that a homogeneous surface charge density is appropriate to describe the electrostatic environment within a CTX II-bound phase, or that POPC trapped within such a phase is able to sample the entire electrostatic environment of that phase, or that the "molecular voltmeter" mechanism functions properly under such circumstances. For POPC remaining in the CTX II-free phase, according to the ^{31}P NMR evidence, no change in lipid ordering is expected. Consequently, the ^{2}H NMR quadrupolar splittings should behave according to the predicted "molecular voltmeter" response. If POPG has a greater affinity for the CTX II-bound phase, then one predicts a decreased anionic surface charge density within the CTX II-free phase. Hence, for

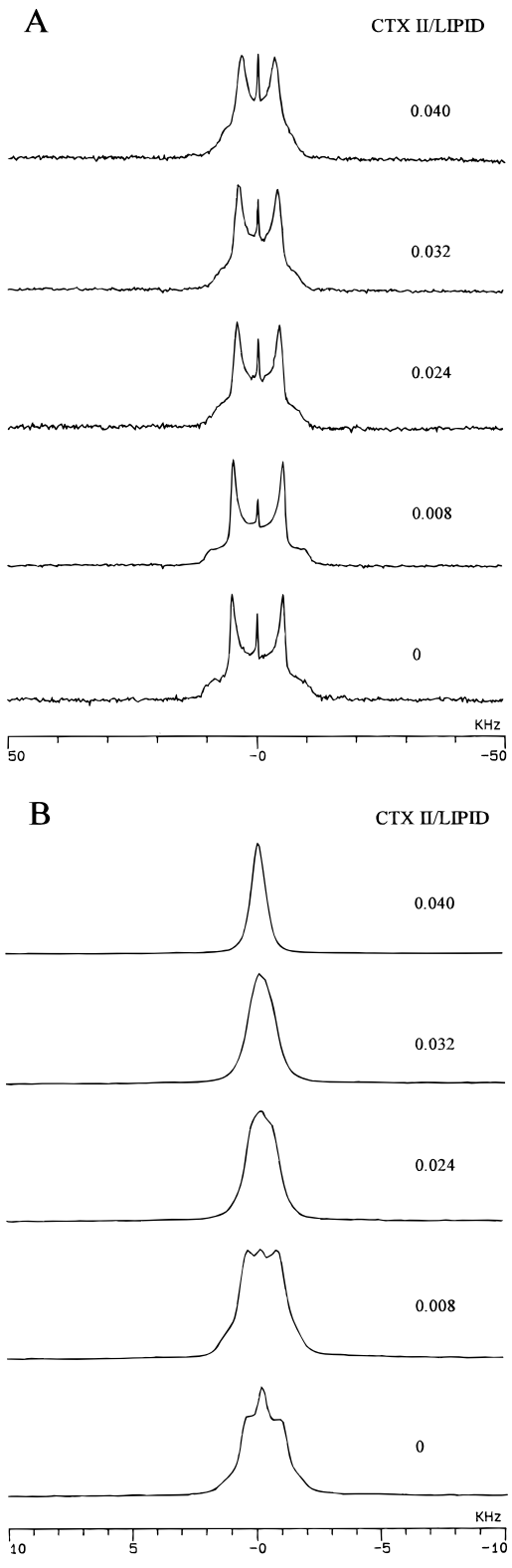

FIGURE 2: Representative ^{2}H NMR spectra from (A) 1:1 POPC-α-d_2/POPG and (B) 1:1 POPC-β-d_2/POPG mixtures in the presence of the following molar ratios of CTX II/total lipid, from bottom to top: 0, 0.8, 2.4, 3.2, and 4.0 mol %.

POPC-α-d_2 the quadrupolar splitting in both phases may well decrease, making it difficult to resolve the two in a ^{2}H NMR spectrum. For POPC-β-d_2 the quadrupolar splitting from the two phases may change in opposite directions, leading one to expect an enhanced resolution of the two environments in the ^{2}H NMR spectrum. However, the quadrupolar splitting from POPC-β-d_2 is less sensitive to surface charge influences than that from POPC-α-d_2. Moreover, in these ^{2}H NMR spectra the digital resolution is about 250 Hz per data point (i.e., a sweep width of 250 kHz digitized into 1024 data points), so that relatively small differences in quadrupolar splittings will not be readily resolved. Furthermore, it may be that the two phases differ with respect to their T_2 relaxation times. In an echo experiment differential relaxation losses may alter the apparent intensity contributions from two (or more) such phases. Both the static ^{31}P NMR and ^{2}H NMR spectra reported here are particularly vulnerable to such effects. An extensive relaxation time study would be useful to confirm the authenticity of the line shapes. For the moment, it appears that ^{2}H NMR of choline-deuterated POPC is not definitive with respect to phase separation of a CTX II-bound phase.

CTX II Binds Preferentially to POPG over POPC. Under fast MAS conditions the ^{31}P NMR spectra of POPC/POPG mixtures consist solely of the isotropic resonance lines of the individual lipids, with no SSB intensity whatsoever. A singular advantage of the fast MAS ^{31}P NMR experiment is that the individual resonances for each phospholipid component in the mixed bilayer can be observed under conditions of high sensitivity and resolution. Signal-to-noise is enhanced because the resonance intensity is not spread over a range of frequencies corresponding to $\Delta\sigma$ but, instead, is focused under the isotropic resonance line. Resolution can be enhanced because the spectral window may be narrowed without danger of "folding-in" of SSBs.

Representative fast MAS ^{31}P NMR spectra are shown in Figures 3A and 4A for 1:1 and 3:1 mixtures of POPC:POPG, respectively, in the presence of the indicated molar ratio of CTX II. In the absence of CTX II (bottom spectra) the spectrum consists of two resonances, corresponding to the resolved isotropic chemical shifts for POPG (0.5 ppm) and POPC (−0.6 ppm). Adding CTX II induces the appearance of two new isotropic resonances shifted approximately 0.5 ppm downfield from the isotropic chemical shifts of POPG and POPC. For instance, in the middle spectrum of figure 3A, for the case of 2.4 mol % CTX II added to 1:1 mixtures of POPC/POPG, there are four overlapping resonance lines visible. As more CTX II is added, the intensity of these "new" POPG and POPC resonances increase while, simultaneously, the intensity of the "old" POPG and POPC resonances decrease. In general, CTX II addition first influences the POPG resonance, while higher concentrations are required to influence the POPC resonance. At high levels of CTX II only the two downfield-shifted resonances remain. Essentially identical effects are observed with either the 1:1 or the 3:1 mixtures of POPC/POPC, albeit at different molar ratios of CTX II.

The downfield shift in the isotropic resonance lines of POPG and POPC clearly relates to their association with CTX II. One may postulate that the altered isotropic chemical shift observed upon association with CTX II arises due to the interaction of the phospholipid headgroups with cationic sites on the protein. Since dehydration of the headgroups must accompany such an interaction, deshielding of the phosphorus nucleus results.

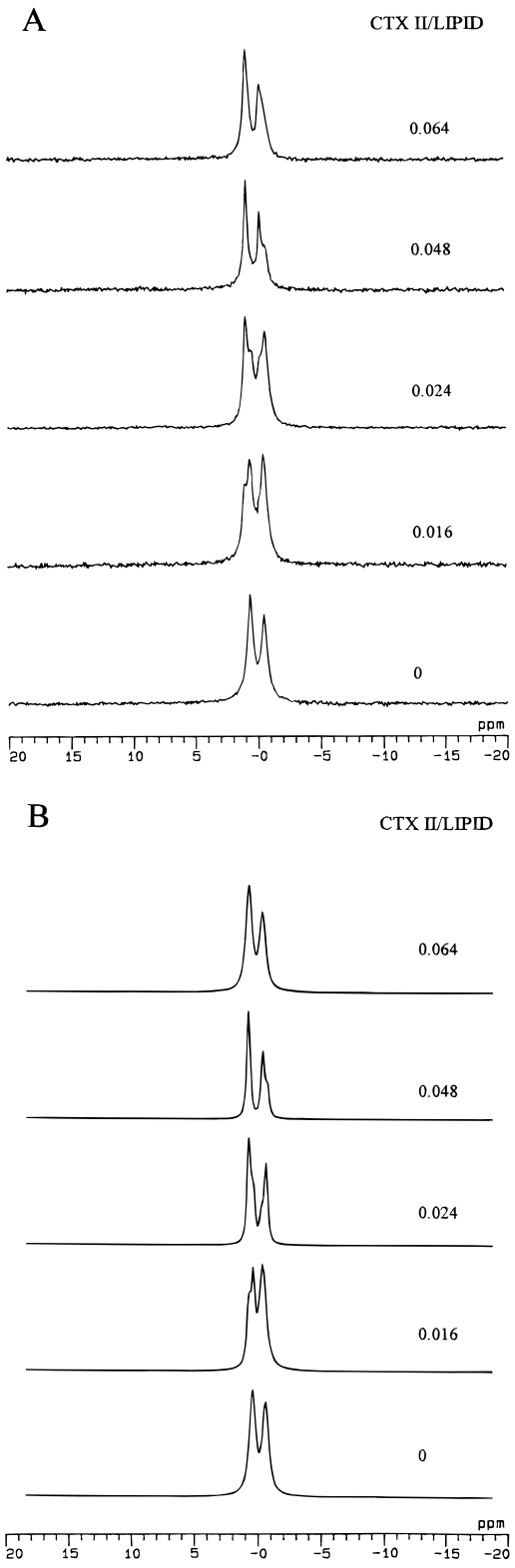

FIGURE 3: (A) Representative fast MAS ^{31}P NMR spectra (frequency of rotation = 6000 Hz) from 1:1 POPC/POPG mixtures in the presence of the following molar ratios of CTX II/total lipid, from bottom to top: 0, 1.6, 2.4, 4.8, and 6.4 mol %. (B) Computer simulations of the ^{31}P NMR spectra in panel A. Details of simulations are described in the text.

For spectra such as those in Figures 3A and 4A, where serious overlap of constituent resonance lines is a complicating factor, quantifying the amounts of POPG and POPC in

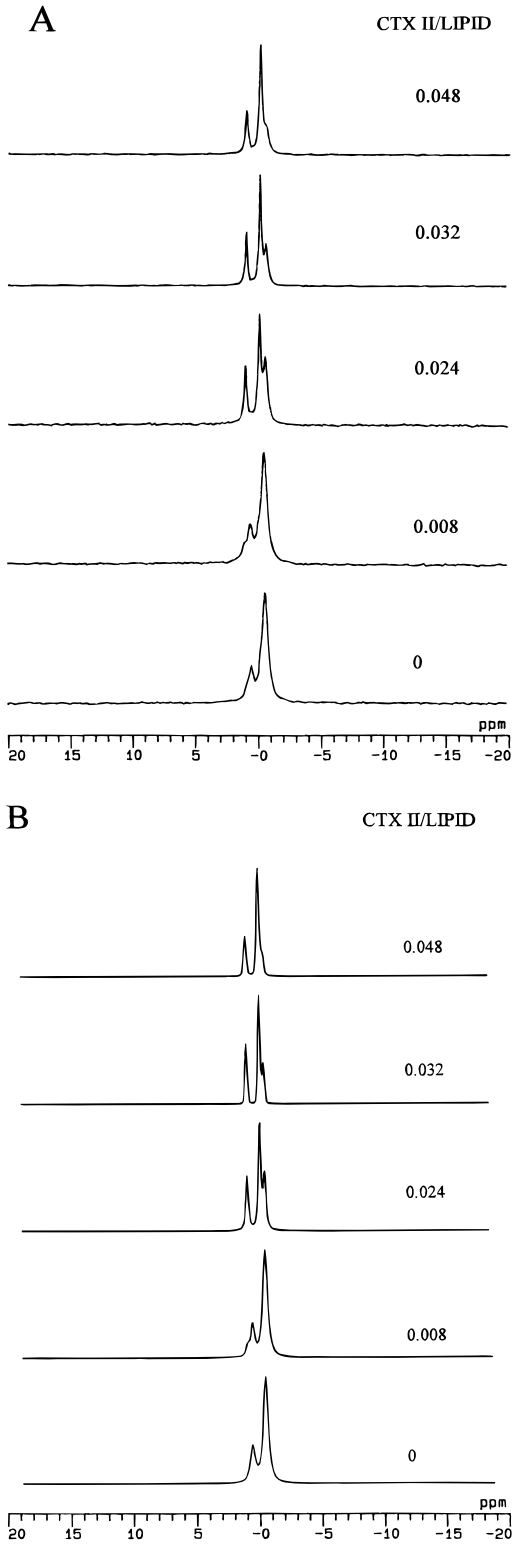

FIGURE 4: (A) Representative fast MAS ^{31}P NMR spectra (frequency of rotation = 6000 Hz) from 3:1 POPC/POPG mixtures in the presence of the following molar ratios of CTX II/total lipid, from bottom to top: 0, 0.8, 2.4, 3.2, and 4.8 mol %. (B) Computer simulations of the ^{31}P NMR spectra in panel A. Details of simulations are described in the text.

the "free" and "CTX II-bound" states is best accomplished by means of a spectral simulation procedure, as detailed in Materials and Methods. Figures 3B and 4B illustrate the spectral simulations for the 1:1 and 3:1 POPC/POPG mixtures, respectively, at CTX II levels corresponding to

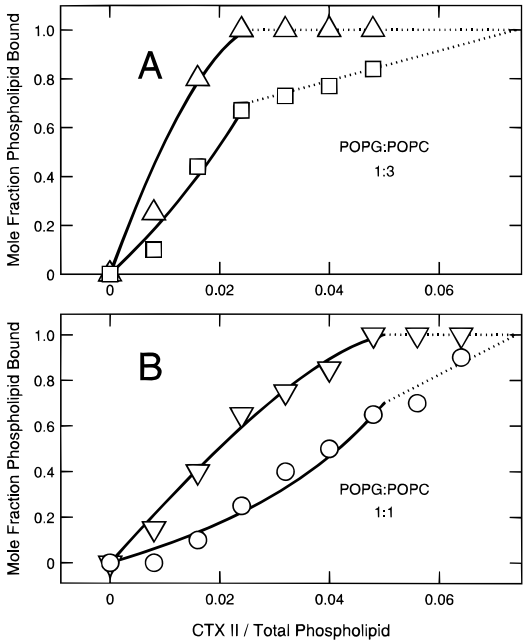

FIGURE 5: Cardiotoxin II−POPG and cardiotoxin−POPC binding isotherms for (A) 3:1 and (B) 1:1 POPC/POPG mixtures. The fraction of bound POPC or POPG is obtained from the normalized amplitude of the corresponding ^{31}P NMR resonance line, as estimated by computer simulations described in the text. The CTX II levels are expressed as a ratio with respect to the total lipid. Symbols: POPC/POPG = 3:1, (△) POPG bound, (□) POPC bound. POPC/POPG = 1:1, (▽) POPG bound, (○) POPC bound. The solid lines correspond to the predictions of the two-site model described in the text for the cases: $B_t/A_t = 1$, $n = 10$, $m = 7$ and $B_t/A_t = 3$, $n = 10$, $m = 21$.

those in Figures 3A and 4A. The simulations assumed the presence of four resonance lines, with isotropic chemical shifts corresponding to POPC and POPG "bound" and "free", these being determined from the "end point" spectra with and without added CTX II. The line shapes of these "end point" spectra were fit with a combination of Lorentzian and Gaussian broadening functions which, once determined, were not allowed to vary for different levels of CTX II. The sole variable becomes, therefore, the relative fraction of "free" and "bound" POPG or POPC. A comparison of Figures 3A and 4A with Figures 3B and 4B shows that the correspondence between the simulated and experimental spectra achieved using this approach is quite satisfactory.

Figure 5 panels A and B illustrate the dependence of the mole fraction of "bound" POPG or POPC, determined by simulation of the fast MAS ^{31}P NMR spectra, as a function of the CTX II/total lipid molar ratio, for 3:1 and 1:1 mixtures of POPC/POPG, respectively. For POPG, the fraction "bound" to CTX II increases directly with the amount of added CTX II and quickly approaches 100%. Not suprisingly, the amount of added CTX II required to achieve 100% POPG "bound" for the 3:1 POPC/POPG mixture is about half that required to achieve 100% "bound" POPG for the 1:1 POPC/POPG mixture. For POPC, the fraction "bound" to CTX II increases slowly with added CTX II and, particularly in the case of the 3:1 POPC/POPG mixture, never reaches 100%. It is evident from these data that CTX II binds preferentially to POPG versus POPC in both 1:1 and 3:1 mixtures of POPC/POPG.

A striking illustration of the preferential interaction of CTX II with POPG is obtained when one plots the mole fraction

of "bound" POPG or POPC as a function of the molar ratio of CTX II/POPG, as shown in Figure 6. Remarkably, the fractions of "bound" POPG and POPC for the 3:1 and 1:1 POPC/POPG mixtures are now superimposed onto "universal" curves for that particular phospholipid species. This demonstrates that the CTX II / POPG ratio is the single factor determining the amounts of "bound" and "free" phospholipid. In the following, we propose a model based on these observations which reproduces the experimental dependence of phospholipid binding levels on the amount of added CTX II and permits one to extract quantitative information from such data regarding the number of phospholipid binding sites per CTX II molecule and the relative affinity for POPG versus POPC.

Statistical-Thermodynamics Model of POPG and POPC Binding to CTX II. Our goal here is to examine different phospholipid−cardiotoxin binding models for their ability to reproduce the experimental binding data presented in Figures 5 and 6. Two models in particular seem plausible and worthy of further examination: a single-site model in which POPG and POPC compete for a finite number of identical sites located on CTX II, and a two-site model in which the different sites display differing relative affinities for POPG versus POPC. Both situations may be modeled starting from statistical-thermodynamic considerations.

(A) Identical Independent Binding Sites. The simplest scenario involves a single type of binding site on CTX II for which POPG and POPC compete. To begin, one invokes a polymeric species C (corresponding to CTX II) having multiple, identical, independent, ligand binding sites for which two different ligands, A (corresponding to POPG) and B (corresponding to POPC), compete. Our experimental observation that CTX II is never found free in solution at any concentration tested in these studies permits us the simplifying assumption that all added C is bound to the membrane and all ligand binding sites are always fully occupied. The question then becomes one of deriving an expression relating the fraction of sites containing A versus B as a function of the amount of added C, the global ratio of A to B, and the relative affinities of A versus B for binding to the available sites.

The association constants for the binding of A or B to any one site on C may be written in the usual fashion.

$$[\mathrm{A}] + [\mathrm{C}] \rightleftharpoons [\mathrm{CA}]; \qquad K = \frac{[\mathrm{CA}]}{[\mathrm{A}][\mathrm{C}]}$$

$$[\mathrm{B}] + [\mathrm{C}] \rightleftharpoons [\mathrm{CB}]; \qquad L = \frac{[\mathrm{CB}]}{[\mathrm{B}][\mathrm{C}]} \tag{1}$$

With the empty ligand binding site providing the reference state, the Gibbs energy of the ligand- bound state equals

$$G_{\mathrm{CA}} = -RT \ln K[\mathrm{A}]$$

$$G_{\mathrm{CB}} = -RT \ln L[\mathrm{B}] \tag{2}$$

For the case of n identical and independent binding sites, the Gibbs' energy of a state having a sites occupied by ligands of type A and $b = n - a$ sites occupied by ligands of type B is therefore defined as follows:

$$G_{\mathrm{A}^a\mathrm{B}^b\mathrm{C}} = G_{ab} = -RT \ln[(K[\mathrm{A}])^a(\mathrm{L}[\mathrm{B}])^b] \tag{3}$$

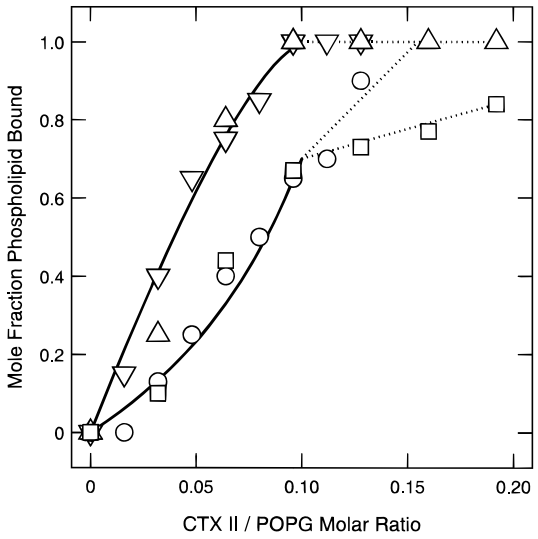

FIGURE 6: Cardiotoxin II−POPG and cardiotoxin−POPC binding isotherms for 3:1 and 1:1 POPC/POPG mixtures. The fraction of bound POPC or POPG is obtained from the normalized amplitude of the corresponding ^{31}P NMR resonance line, as estimated by computer simulations described in the text. The CTX II levels are expressed as a ratio with respect to POPG only. Symbols: POPC/POPG = 3:1, (△) POPG bound, (□) POPC bound. POPC/POPG = 1:1, (▽) POPG bound, (○) POPC bound. The solid line corresponds to the predictions of the two-site model described in the text for the cases: $B_t/A_t = 1$, $n = 10$, $m = 7$ and $B_t/A_t = 3$, $n = 10$, $m = 21$. In this representation the predictions of the model for the two ratios of POPC/POPG overlap.

The probability of the occurrence of any one state $\mathrm{A}^a\mathrm{B}^b\mathrm{C}$ is defined according to the partition function for the situation under consideration.

$$P_{ab} = \frac{g_{ab} \exp[-G_{ab}/RT]}{\sum_{a=0}^{n} g_{ab} \exp[-G_{ab}/RT]} \tag{4}$$

Here g_{ab} is the statistical weight for a given state and is defined as follows:

$$g_{ab} = \frac{n!}{a!(n-a)!} \tag{5}$$

Substituting eq 3 into eq 4, letting $R = K[\mathrm{A}]$ and $S = L[\mathrm{B}]$, and employing the binomial theorem yields the following redefinition of the state probability:

$$P_{ab} = \left[\frac{n!}{a!(n-a)!}\right]\left[\frac{R^a S^{n-a}}{(R+S)^n}\right] \tag{6}$$

The average number of ligands of type A or B bound per molecule of C may then be calculated using

$$\langle a \rangle = \sum_{a=0}^{n} a P_{ab} = \frac{nR}{R+S}$$

$$\langle b \rangle = \sum_{b=0}^{n} b P_{ab} = \frac{nS}{R+S} \tag{7}$$

The total number of bound ligands of type A or B for a given level of added C is then simply the average number bound per molecule of C times the number of added C. For

comparison with our experimental data it is convenient to express the binding in terms of mole fractions. For the case $K > L$ one may show

$$2X_b^A = 2\frac{A_b}{A_t} = \left[\frac{nC}{A_t}\right] + \left[\frac{1+Q}{1-L/K}\right] - \left[\left(\frac{nC}{A_t}\right)^2 - 2\left(\frac{nC}{A_t}\right)\left(\frac{1-Q}{1-L/K}\right) + \left(\frac{1+Q}{1-L/K}\right)^2\right]^{1/2} \quad (8)$$

$$2X_b^B\left(\frac{B_t}{A_t}\right) = 2\frac{B_b}{B_t}\left(\frac{B_t}{A_t}\right) = \left[\frac{nC}{A_t}\right] - \left[\frac{1+Q}{1-L/K}\right] + \left[\left(\frac{nC}{A_t}\right)^2 - 2\left(\frac{nC}{A_t}\right)\left(\frac{1-Q}{1-L/K}\right) + \left(\frac{1+Q}{1-L/K}\right)^2\right]^{1/2} \quad (9)$$

where the subscripts b and t refer to bound and total, and $Q = LB_t/KA_t$. Note that the only fitting variables in these two equations are the molar ratio of the two types of ligands, B_t/A_t, and the relative affinities of the two ligands for the binding sites, L/K. In deriving eqs 8 and 9, we have employed the assumption that all sites have ligand bound, from which it follows that $A_b + B_b = nC$.

This single-site model fails to reproduce the binding data in Figures 5 and 6. Specifically, only for the case $K \gg L$ do the POPG binding curves for the two POPC/POPG molar ratios 1:1 and 3:1 superimpose when plotted as a function of C/A_t. Under these circumstances eqs 8 and 9 reduce to

$$X_b^A = \left[\frac{nC}{A_t}\right]; \quad X_b^B = 0 \quad (10)$$

The difficulty then is that for $K \gg L$ the single-site model predicts no POPC binding whatsoever.

(B) Nonidentical Independent Binding Sites. Much greater success at reproducing the experimental binding curves in Figures 5 and 6 is achieved using a model which presumes the existence of two classes of multiple, independent, binding sites. One class of binding site is considered to possess a very high affinity for A and a low affinity for B due to specific electrostatic interactions, such as those occuring between the cationic lysine amino acid side chains of CTX II and anionic lipids such as POPG. The second class of binding site is considered to involve rather less-specific protein−phospholipid interactions, so that both POPG and POPC might occupy such sites with roughly equal affinity. However, it is assumed that, experimentally, one cannot distinguish between phospholipids bound to high-specificity versus low-specificity sites, but only between phospholipids which are "bound" versus "free".

As previously, the amount of bound ligand is simply the average number of ligands bound per molecule of C times the number of added C,

$$A_b = C[\langle a\rangle_H + \langle a\rangle_L]$$

$$B_b = C[\langle b\rangle_H + \langle b\rangle_L] \quad (11)$$

where the subscripts H and L refer to the high and low specificity sites, respectively. In the most general case for two different ligands and two different classes of binding site, one needs to consider four association constants. However, the single-site model discussed above has taught us that for the high-specificity binding sites only the situation $K \gg L$ needs to be considered, so that eqs 10 apply. Moreover, for the low-specificity sites it is reasonable to assume that the association constants for A and B are similar. Consequently, the mole fractions of bound A or B are found to equal

$$X_b^A = \left(\frac{nC}{A_t}\right) + \left(\frac{mC}{A_t}\right)\left[\frac{1 - nC/A_t}{1 + B_t/A_t - nC/A_t}\right]$$

$$X_b^B = \left(\frac{mC}{A_t}\right)\left[\frac{1}{1 + B_t/A_t - nC/A_t}\right] \quad (12)$$

where n and m are the number of binding sites of type H and L, respectively, and all other terms have been defined previously. Note that these expressions apply in the limit $0 \le X_bA \le 1$.

The solid lines in Figures 5 and 6 were obtained using eqs 12 with the fit parameters $B_t/A_t = 1$, $n = 10$, $m = 7$ and $B_t/A_t = 3$, $n = 10$, $m = 21$. Clearly one may reproduce the experimental binding data using this two-site model, but do the parameters so obtained make sense? Previous studies of phospholipid binding to CTX II have all deduced a stoichiometry of 8−10 cationic charges per CTX II (Batenburg *et al*., 1985). Our finding that the number of high-specificity binding sites is $n = 10$ agrees well with these earlier studies. The fact that n does not vary with the ratio B_t/A_t is a consequence of the specificity of these sites for POPG, reflecting the strong electrostatic attraction between the anionic ligand and the fixed number of cationic binding sites. The number of low-specificity binding sites m does vary with the ratio B_t/A_t, and this suggests that such sites might not correspond to direct protein−phospholipid contact sites. Instead, it is reasonable to suppose that the presence of CTX II affects the physical properties of lipids in its vicinity in some indirect fashion, so that the number of such lipids is not fixed. Although it may be entirely circumstantial, it is nevertheless compelling to discover that the number of such low-specificity binding sites m triples when the ratio of low affinity to high-affinity phospholipid triples.

At CTX II concentrations sufficient to bind 100% of the POPG, only 70% of the POPC is bound. Equations 12 no longer apply, however, and further POPC binding proceeds in a linear fashion with increasing CTX II/POPG, as shown by the dashed lines in Figure 5B. The proportionality constants for the 1:1 and 3:1 POPC/POPG mixtures differ by a factor B_t/A_t. This suggests that further CTX II binding to the lipid bilayer does occur after POPG is 100% neutralized, implying a hydrophobic component to the attraction felt by CTX II for membrane surfaces.

The two nonidentical, independent, binding sites model is the simplest model to successfully describe the CTX II−phospholipid binding data. Other, more sophisticated models can be envisaged. In particular, the binding data themselves manifest a degree of sigmoidal behavior, suggesting a departure from the assumption of independent sites. However, sigmoidal behavior is always most evident at the extremes of nearly 100% bound or 100% free. Unfortunately, given the overlap between the bound and free resonances in the ^{31}P NMR spectra, at these extremes quantification of the minor component is least reliable. As a consequence, we judge that more sophisticated modeling is not warranted.

CONCLUDING REMARKS

Early studies of CTX II (Dufourq & Faucon, 1978: Vincent *et al*., 1978) showed that basic residues on the protein interact specifically and quantitatively with the anionic polar headgroups of phospholipids. When the anionic phospholipid is cardiolipin, CTX II binding is accompanied by formation of an inverted micellar phase (Batenburg *et al*., 1985), a reflection of cardiolipin's well-known tendency to assume nonbilayer-phase structures (Cullis *et al*., 1978: de Kruijff & Cullis, 1980). However, the high affinity of cardiotoxins for anionic lipids ($K_d < 10^{-7}$ M) is not sufficiently explained by ion-pair formation alone. Recent evidence (Chien *et al*., 1994) demonstrates that hydrophobic interactions reinforce the initial electrostatic interaction occuring between cardiotoxins and lysophosphatidylcholine micelles. Faucon *et al*. (1983) and Batenburg *et al.* (1985) suggest that CTX II inserts its hydrophobic β-pleated sheet into the interior of the bilayer membrane. FTIR studies by Surewicz *et al*. (1988) indicate that the β-sheet content of CTX II increases upon binding to phosphatidylglycerol.

The results presented here confirm that CTX II interacts with high specificity with a monovalent anionic phospholipid, POPG. The "free" phospholipid not interacting with CTX II becomes depleted with respect to POPG. The specificity of CTX II for POPG does not appear to be absolute, in that POPC also interacts with CTX II. Thus, it is not possible to draw conclusions regarding the segregation of POPC from POPG within the "bound" state. It is possible, nevertheless, to conclude that CTX II preferentially withdraws POPG from the "free" state. Our findings indicate further that the resulting membrane architecture is not necessarily nonbilayer. Specifically, the observed residual chemical shift anisotropy for POPG and POPC interacting with CTX II is consistent with a decreased order parameter for the phospholipid polar headgroup, or possibly a reorientation, rather than a transition to a nonbilayer architecture.

The present study highlights the advantages of MAS ^{31}P NMR for observing lipid−protein interactions. In particular, it has proved possible to differentiate and quantify the specificity of interactions with particular phospholipids without the necessity of isotopic labeling or the complications inherent in bulky spin labels. The quality of the data was such that its was possible to develop and test different statistical-thermodynamics models to explain the observations. The approach developed here is quite general, and it should be possible to adapt the statistical-thermodynamics model(s) to other surface-seeking proteins, even when binding to membrane surfaces is not quantitative. For the case of CTX II the models indicate the presence of two classes of binding site, corresponding to high and low specificity for POPG.

Many cationic surface-seeking proteins also show a preference for anionic lipids. Melittin, for example, binds preferentially to negatively charged lipid bilayer surfaces (Dufourq & Faucon, 1977). Using ^{31}P NMR, Monette and Lafleur (1995) observed a decrease in melittin-induced lysis in DMPC/DMPG vesicles with increasing DMPG content. They propose that this is due to electrostatic anchoring of melittin at the membrane surface which inhibits its ability to penetrate to the membrane interior, a step necessary for lysis to occur. On the other hand, melittin does not appear able to sequester anionic lipids (Beschisaschvili & Seelig, 1990), possibly because of it relatively small size. However, its effective charge of +2 when bound at the membrane surface is lower than the formal charge of +5 calculated from melittin's amino acid sequence (Beschiaschvili & Seelig, 1990). In contrast, the 21 amino acid, surface-seeking peptide P828 studied by Gawrisch *et al.* (1995) contains six arginine residues and is able to sequester phosphatidylglycerol from mixtures with phosphatidylcholine, while maintaining an overall lamellar bilayer structure.

Cytochrome *c* is much larger than melittin, binds preferentially to anionic lipid bilayers (de Kruijff & Cullis, 1980: Demel *et al*., 1989; Choi & Swanson, 1995), and sequesters cardiolipin from the midst of mixtures with phosphatidylcholine plus phosphatidylethanolamine (Pinheiro & Watts, 1994). Cytochrome *c* binding to cardiolipin induces a nonbilayer phase, while binding to other anionic lipids such as phosphatidylglycerol or phosphatidylserine does not (de Kruijff & Cullis, 1980; Devaux & Seigneuret, 1985). In this sense cytochrome *c* and CTX II appear rather similar. An important difference between cytochrome *c* and cardiotoxin II is that, at the ionic strengths employed here, cytochrome *c* is in only partially bound to the membrane surface (Heimburg & Marsh, 1995), while CTX II binding is apparently quantitative. Moreover, the effective charge on cytochrome *c*, deduced by Heimburg and Marsh (1995) from their binding studies, is only +3 to +4, rather than the value of +9 anticipated from the amino acid sequence. The amino acid sequence of CTX II leads one to expect an overall charge of +10, and indeed the stoichiometry of POPG binding by CTX II confirms that this is the effective charge. Thus, it appears that overall effective cationic charge is the best predictor of the ability to sequester anionic lipids.

We have no simple explanation for the physical origin of the high- versus low-specificity lipid binding sites suggested by our models. If direct CTX II−POPC contact sites constitute the low-specificity binding sites, it is not obvious why the number of low-specificity sites *m* should vary with the ratio POPC/POPG. The answer may lie, not in specific protein−lipid contacts, but in some more global physical effect. One possibility is that the aggregation state of CTX II within the plane of the membrane differs as a function of the POPC/POPG ratio. In their statistical-thermodynamic model of protein aggregation at membrane surfaces, Heimburg and Marsh (1995) predict a lower number of bound lipids per protein for cytochrome *c* in an aggregated versus dispersed state, although they considered only 100% anionic phospholipid membranes. It is equally possible, however, that the influence of CTX II on its lipid environment extends beyond its immediate vicinity to an extent that, in these studies, is still limited by the availablity of POPC.

Currently, the aggregation state of CTX II under these, or any other, circumstances remains unknown.

REFERENCES

Aloy, M., & Rabaut, C. (1913) *Bull. Soc. Chim. Fr. 13*, 457−460.

Aneja, R., Chada, J., & Davies, A. (1970) *Biochim. Biophys. Acta 218*, 102−111.

Batenburg, A., Bougis, P., Rochat, H., Verkleij, A., & de Kruiff, B. (1985) *Biochemistry 24*, 7101−7110.

Beschiaschvili, G., & Seelig, J. (1990) *Biochemistry 29*, 52−58.

Bougis, P., Rochat, H., Pieroni, G., & Verger, R. (1981) *Biochemistry 20*, 4915−4920.

Bougis, P., Marchot, P., & Rochat, H. (1986) *Biochemistry 25*, 4915−4920.
Chien, K., Chiang, C., Hseu, Y., Vyas, A., Rules, G., & Wu, W. (1994) *J. Biol. Chem. 269*, 14473−14483.
Choi, S., & Swanson, J. (1995) *Biophys. Chem. 54*, 271−278.
Cullis, P., Verkeij, A., & Ververgaert, P. (1978) *Biochim. Biophys. Acta 513*, 11−20.
Dauplais, M., Neumann, J., Pinkasfeld, S., Menz, A., & Roumestand, C. (1995) *Eur. J. Biochem. 230*, 213−220.
Davis, J., Jeffrey, K., Bloom, M., Valic, M., & Higgs, T. (1976) *Chem. Phys. Lett. 42*, 390−394.
de Kruijff, B., & Cullis, P. (1980) *Biochim. Biophys. Acta 602*, 477−490.
Demel, R., Jordi, W., Lambrechts, H., van Damme, H., Hovius, R., & de Kruijff, B. (1989) *J. Biol. Chem. 264*, 3988−3997.
Désormeaux, A., Laroche, G., Bougis, P., & Pézolet, M. (1992) *Biochemistry 31*, 12173−12182.
Devaux, P., & Seigneuret, M. (1985) *Biochim. Biophys. Acta 822*, 63−125.
Dufourcq, J., & Faucon, J. (1977) *Biochim. Biophys. Acta 467*, 1−11.
Dufourcq, J., & Faucon, J. (1978) *Biochemistry 17*, 1170−1176.
Dufourcq, J., Faucon, J., Bernard, E., Pézolet, M., Tessier, M., Bougis, P., Van Rietschoten, J., Delori, P., & Rochat, H. (1982) *Toxicon 20*, 165−174.
Faucon, J., Dufourcq, J., Bernard, E., Duchesneau, L., & Pézolet, M. (1983) *Biochemistry 22*, 2179−2185.
Fryklund, L., & Eaker, D. (1975) *Biochemistry 14*, 2860−2865.
Gawrisch, K., Barry, J., Holte, L., Sinnwell, T., Bergelson, L., & Ferretti, J. (1995) *Mol. Membr. Biol. 12*, 83−88.
Griffin, R. (1981) *Methods Enzymol. 72*, 108−174.
Harbisson, G., & Griffin, R. (1984) *J. Lipid Res. 25*, 1140−1142.
Harvey, A., Marshall, R., & Karlsson, E. (1982) *Toxicon 20*, 379−396.
Heimburg, T., & Marsh, D. (1995) *Biophys. J. 68*, 536−546.
Herzfeld, J., & Berger, A. (1980) *J. Chem. Phys. 73*, 6021−6030.
Karlsson, E., Arnberg, H., & Eaker, D. (1971) *Eur. J. Biochem. 21*, 1−16.
Kates, M. (1972) *Techniques in Lipidology*, North Holland, Amsterdam.
Louw, A. (1974) *Biochim. Biophys. Acta 336*, 470−480.
Macdonald, P. M., Leisen, J., & Marassi, F. M. (1991) *Biochemistry 30*, 3558−3566.
Marassi, F., & Macdonald, P. (1992) *Biochemistry 31*, 10031−10036.
Marassi, F., Djukic, S., & Macdonald, P. (1993) *Biochim. Biophys. Acta 1146*, 219−228.
Monette, M., & Lafleur, M. (1995) *Biophys. J. 68*, 187−195.
Nikolelis, D., Brennan, J., Brown, S., & Krull, U. (1992) *Anal. Chim. Acta 257*, 49−57.
Pézolet, M., Duchesneau, L., Bougis, P., Faucon, J., & Dufourcq, J. (1982) *Biochim. Biophys. Acta 704*, 515−523.
Pinheiro, T., & Watts, A. (1994) *Biochemistry 33*, 2459−2467.
Rance, M., & Byrd, R. (1983) *J. Magn. Reson. 52*, 221−240.
Rees, B., & Bilwes, A. (1993) *J. Am. Chem. Soc. 6*, 385−406.
Seelig, J. (1978) *Biochim. Biophys. Acta 515*, 105−140.
Seelig, J., Macdonald, P., & Scherer, P. (1987) *Biochemistry 26*, 7535−7541.
Singhal, A., Chien, K., Wu, W., & Rule, G. (1993) *Biochemistry 32*, 8036−8044.
Surewicz, W., Stepanik, T., Szabo, A., & Mantsch, H. (1988) *J. Biol. Chem. 263*, 786−790.
Vincent, M., Balerna, M., & Lazdunski, M. (1978) *FEBS Lett. 85*, 103−108.

BI952349I